



# Analysis of influencing factors for the dressing process in double side face grinding

Eckart Uhlmann<sup>1,2</sup> · Linus Lichtschlag<sup>1</sup>

Received: 3 August 2020 / Accepted: 15 December 2020 / Published online: 4 January 2021  
© The Author(s) 2021

## Abstract

In grinding, the design of the dressing process is an essential part of work preparation and restoration of the grinding wheel's profile and cutting ability. In contrast to most grinding processes, the choice of dressing parameters in double face grinding with planetary kinematics has so far only been experience-based. As a consequence, the dressing process causes a higher degree of tool wear than the machining of the workpieces. A focused design of the dressing process based on a scientific data could help to improve the ecological and the economic efficiency by reducing tool wear and the amount of dressing tools used. In this paper, methods for determining the wear condition and the result of the dressing process, including macro- and microscopic characteristic are presented. This includes a correlation analysis between parameters of wear characteristics and workpiece surface quality. Furthermore, technological investigations are carried out in order to systematically limit the main influencing factors on the dressing process. As a result, the parameters dresser grain size  $d_{gd}$ , rotational speed ratio  $n_{ld}$  and the machined dresser height  $\Delta h_d$  are identified as significant for dressing. The knowledge about their principal influence on the dressing result could provide the basis for further research.

**Keywords** Double face grinding with planetary kinematics · Tool wear determination · Dressing process · Profiling and sharpening of grinding wheels

## 1 Introduction

Grinding wheel wear is a decisive factor in terms of economy and workpiece quality. The profile and cutting ability must be generated and maintained using suitable conditioning strategies. While extensive knowledge of these processes is already available for other grinding processes, only initial approaches have been published to date for double face grinding with planetary kinematics. The substitution of double-sided face lapping processes by double-sided grinding processes to reduce the environmental impact and increase the economic efficiency requires a deepening of the process knowledge. Double face grinding with planetary kinematics is a manufacturing process that is used for machining plane-

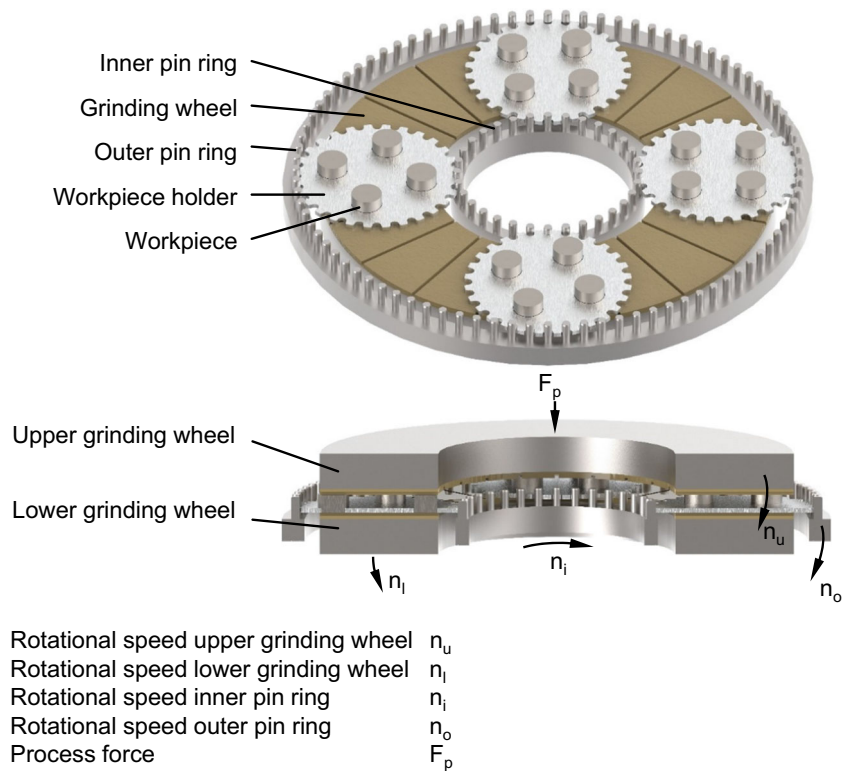
parallel surfaces. It is used in the production of e.g. metallic bearing rings, ceramic workpieces, such as sealing and control discs, and elements of optical systems. The advantages of the process are the high achievable surface quality and low achievable flatness errors, which result from the special kinematics in the form of overlapping machining tracks. Compared to lapping, the environmental impact is lower due to the longer endurance of the grains bound in grinding wheels. Furthermore, cooling lubricant is reusable through filtration. In addition, the workpieces require less cleaning after machining. A characteristic feature of the process is the double-sided, non-continuous batch production of the workpieces. The kinematics and arrangement of the tools are similar to double-sided face lapping with forced guidance from which the double face grinding with planetary kinematics originated. The machine structure consists of two horizontally arranged grinding wheels, between which the workpieces are inserted unclamped into externally toothed workpiece holders (Fig. 1). The workpiece holders are guided by a driven inner pin ring and usually stationary outer pin ring. During machining, the workpieces perform cycloidal movements in relation to the grinding wheel surface. These movements result from

✉ Linus Lichtschlag  
linus.lichtschlag@iwf.tu-berlin.de

<sup>1</sup> Institute for Machine Tools and Manufacturing (IWF), Technische Universität Berlin, Pascalstrasse 8 – 9, 10587 Berlin, Germany

<sup>2</sup> Fraunhofer Institute for Production Systems and Design Technology (IPK), Pascalstrasse 8 – 9, 10587 Berlin, Germany

**Fig. 1** Main components of the machine system for double face grinding with planetary kinematics [5]



the overlapping of the driven grinding wheels, the rotation of the inner pin ring and the eventuating workpiece holder rotation. Due to the planar contact of the grinding wheels, the surfaces of a workpiece are evenly loaded [1–5].

## 2 Fundamental theory

The relative movement between the workpieces and grinding wheels results in different cutting speeds  $v_c$  on the inside and outside of the grinding wheels. Furthermore, the workpieces cover different path lengths in the inner and outer area of the abrasive surface. This combination of radially dependent cutting speed  $v_c$  and contact length of the workpieces with the grinding wheel follows in inhomogeneous wear of the grinding wheels. They are affected by macro- and microscopic wear. Macroscopic deviations from the even grinding surface result in reduced workpiece flatness. Microscopic wear in the form of grain blunting and bond failure has a decisive influence on the economic efficiency and workpiece quality of the production process. Both types of wear need to be minimized by suitable dressing processes [5–9].

Due to the kinematic relationship between the double face grinding with planetary kinematics and the double-sided face lapping with forced guidance, the same macroscopic wear characteristics occur in the inner and outer area of the grinding wheels. Simpfendörfer [10] divides the forms of wear into 0<sup>th</sup> and 1<sup>st</sup> order (Fig. 2). The wheel shape for 0<sup>th</sup> order defects is

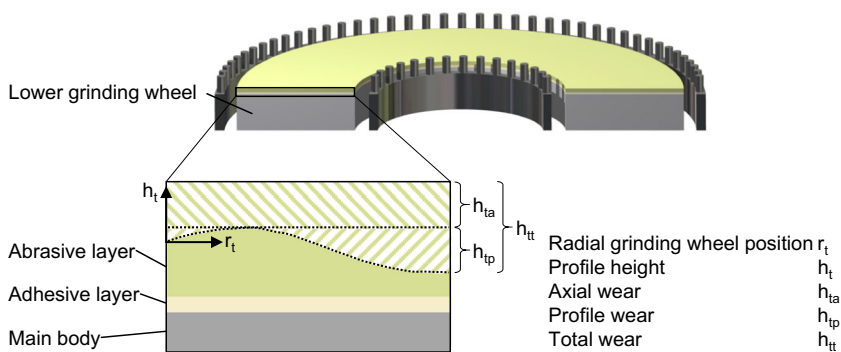
characterized by concave or convex characteristics over the entire tool surface. In contrast, 1<sup>st</sup> order errors have a convex or concave characteristic within the area between the inner and outer edge of the tool [3, 10].

Based on the work of Sabotka [11], Funck [12], Ardelt [3] and Stähli [13, 14], Uhlmann et al. [15] define the total wear  $h_{tt}$  that it is composed of the axial wear  $h_{ta}$  and the profile wear  $h_{tp}$  (Fig. 3). Here, the profile height  $h_t$  over the radial grinding wheel position  $r_t$  describes the macroscopic wear characteristic based on a coordinate system located on the outer tool

| Defect order | axial direction | wheel shape |
|--------------|-----------------|-------------|
| 0.           | +               |             |
|              | -               |             |
| 1.           | +               |             |
|              | -               |             |

**Fig. 2** Radial wear on lapping wheels [10]

**Fig. 3** Wear characteristics for double face grinding with planetary kinematics [5]



radius. Thus, the profile wear  $h_{tp}$  is the difference between the maximum and the minimum of the profile and represents the target value to be minimized in profiling processes.

The resulting microscopic wear is characterized by the wear of the abrasive grains and the bond in which the grains are held. After profiling, the bond can be reset by appropriate sharpening processes so that underlying grains are exposed and are available for workpiece machining. In grinding, the conditioning processes of profiling and sharpening are usually carried out separately and one after the other [8]. For example, Funck [12] used single- and multi-grain dressers to profile grinding wheels in double face grinding with planetary kinematics with ceramic bonded silicon carbide (SiC) grains. He then used discs of SiC, placed in the holders instead of the workpieces, for sharpening. In the grinding processes that followed, a low but constant material removal rate  $\Delta\dot{h}_w$ , the time-related workpiece height reduction, was achieved within a short time. Ardelt [3] and Uhlmann et al. [16, 17] also used separate profiling and sharpening processes in their investigations into process behaviour and the achievable workpiece quality. Profiling was carried out by using construction steel, which was inserted into the workpiece holders instead of the workpieces. Larger unevenness of the grinding wheel surface was profiled with SiC dressing rings with a grain size of 80 mesh. Reproducible sharpening was also achieved with these dressing rings at constant dressing parameters. However, it is not possible to make a statement about individual influencing variables on the basis of the publications [3, 16, 17]. In Egger’s [18] investigations into the interaction mechanisms between workpiece and tool, sharpening was carried out with bonded and unbonded

grains. The grinding wheels used with a specification of D91 C100 in a ceramic bond were sharpened in the unbound version with a suspension of cooling lubricant, boron carbide ( $B_4C$ ) and SiC grains of size 80 mesh and a steel disc as counterpart. However, sharpening with ceramic-bonded SiC grains in dressing rings showed significantly higher material removal rates  $\Delta\dot{h}_w$  in the subsequent grinding processes. The variation of the dressing pressure  $p_{ed}$  showed a slight influence on the dressing result with a subsequent tendency to more effective machining at lower dressing pressures. Dressing with electroplated single-layer bonded diamond dressers with a grit size D91 also led to a reduced material removal rate  $\Delta\dot{h}_w$ . The reason for this was the inability of the bonded diamond grains to reset the abrasive coating’s bond. Furthermore, the contact of the dressing and grinding diamond grains leads to wear of the dressing and grinding wheels [18]. In the work preparation of the grinding wheels D46 to D126 with C75 to C100 in a ceramic bond, Rußner [19] also used SiC dressing rings for profiling. The subsequent sharpening was carried out with corundum dressers with grain size 80 mesh for all grinding wheels used. Since no parameter variation took place here, no conclusions can be drawn about individual influencing variables [19]. In industrial applications, combined profiling and sharpening processes have become established, which in principle correspond to a mere sharpening process. Here, bonded grains are used in dressing rings or dressing stones, which are inserted into corresponding workpiece holders instead of the workpieces (Fig. 4). Subsequently, the dressing process is the same as for workpiece machining, but the cut dressing ring material forms an emulsion with the cooling lubricant, similar to

**Fig. 4** Dressing rings in the working area of the test machine DLM 505 HS, Stähli AG, Pieterlen/Biel, Switzerland

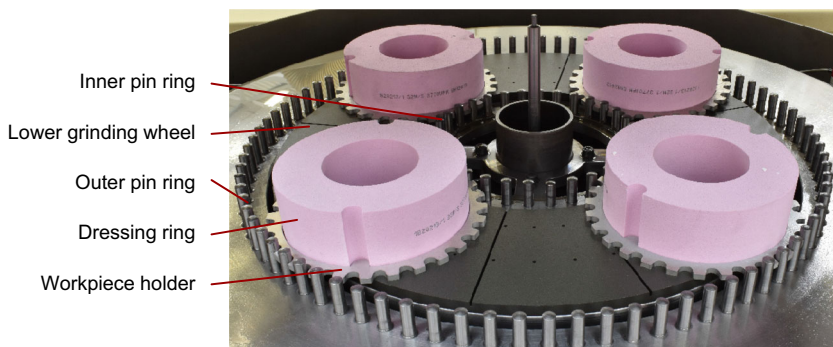
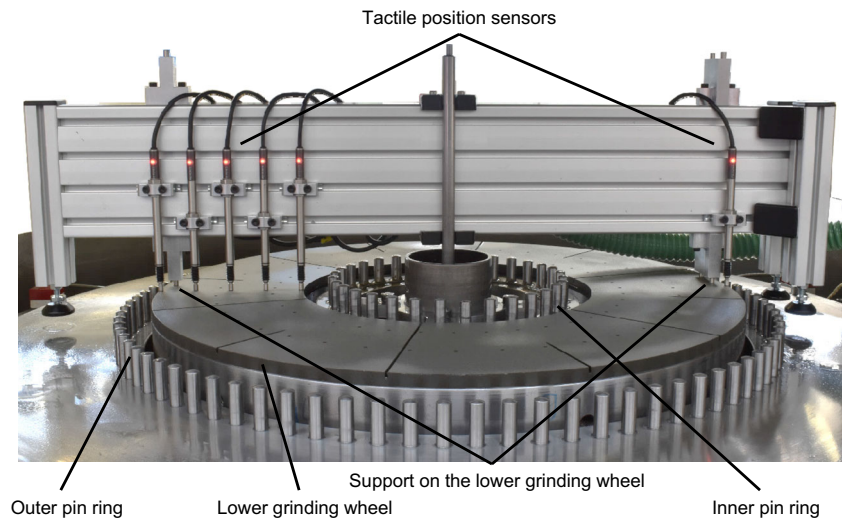


**Fig. 5** Measuring system to determine grinding wheel profile placed on the lower grinding wheel



lapping, which affects the grinding surfaces and thus dresses them. The generation of the even grinding wheel profiles, the profiling, is realized by selecting a favourable rotational speed ratio  $n_{ld}$ , thus the trajectory shape and the targeted higher load of the grinding wheel areas to be levelled [1, 20].

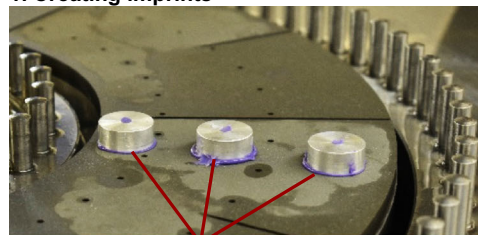
### 3 Determination of wear condition

For the investigation of wear mechanisms and dressing strategies as well as in industrial applications, the reliable determination of the macro- and microscopic wear is necessary. Due to the nature of the process, this can only be realized as a post-

process measurement. Here a self-developed measuring system is used to measure the grinding wheel profiles and to detect the profile wear  $h_{tp}$ . This system consists of six tactile position sensors mounted on a profile rail to determine the profile heights at defined points (Fig. 5). For offset compensation, this is positioned on a standardized flat granite block and zeroed via control software. Then the measuring system is placed on the lower grinding wheel. The measuring section is defined by one sensor each on the outer and inner edge of the grinding wheel. Three further sensors are mounted equidistantly between these. The sixth sensor is positioned on the opposite outer edge and used for horizontal compensation. Assuming a purely radius-dependent wear characteristic, the

**Fig. 6** Topography analysis procedure with imprint creation and measuring

#### 1. Creating imprints



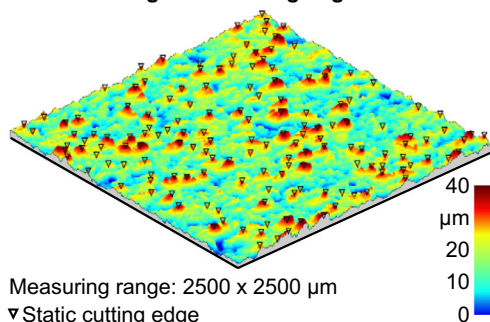
Inner, middle and outer imprint position on the lower grinding wheel

#### 2. Optical measurement



White light interferometer  
Imprints

#### 3. Determining static cutting edges



#### 4. Evaluation of topography parameters

| Parameter                                 |
|---|
| Reduced peak height $S_{pk}$              |
| Reduced valley depth $S_{vk}$             |
| Maximum height $S_z$                      |
| Mean arithmetic height $S_a$              |
| Static number of cutting edges $N_{stat}$ |
| Static cutting edge density $C_{stat}$    |

**Table 1** Process parameters of the blunting process

| Influencing variable                              | Unit                    | Value |
|---|-------------------------|-------|
| Rotational speed of lower grinding wheel $n_{lo}$ | l/min                   | 125   |
| Rotational speed of upper grinding wheel $n_{up}$ | l/min                   | – 250 |
| Process force $F_p$                               | daN                     | 250   |
| Lubricant flow rate $\dot{V}_1$                   | l/min                   | 45    |
| Lubricant   | Grinding Oil Rhenus DP5 |       |

measured values of the two sensors positioned on the outer edge must be identical. If there is a difference and thus tilt between the ideally flat grinding wheel surface and the longitudinal axis of the measuring system, a compensation line is calculated and the measured values corrected. The use of a 4<sup>th</sup> degree polynomial as an approximation of the wheel profile turned out to be sufficiently accurate during measurements and in relation to previously published wear forms [1, 3, 5, 6, 10]. By measuring at different angular positions on the grinding wheel, wear characteristics dependent on the circumference can be determined. To determine the profile of the upper grinding wheel, the measuring system is positioned rotated by 180° so that the sensors point upwards. The upper grinding wheel is then lowered onto these for measurement. The measuring accuracy can be estimated to  $p_{wm} < 10 \mu\text{m}$  when using a test plate according to DIN 876 [21] with a flatness tolerance of  $4 \mu\text{m}/1000 \text{mm}$  and sensors with a repeatability of  $p_{ws} < 1 \mu\text{m}$  [1, 3, 10, 21, 22].

The wear condition of the grinding wheel can be inferred from the workpiece roughness. Lower roughness values Ra and Rz indicate a blunting of the grinding wheel at constant machining parameters. In addition to this indirect method, the determination of parameters of the grinding wheel topography is established. For this purpose, imprints are taken from the grinding wheel topography using the dental imprint material Panasil® contact plus X-Light of Kettenbach GmbH & Co. KG, Eschenburg, Germany. One imprint each is made on the inner and outer edge and in the middle between them on the lower and upper grinding wheel (Fig. 6). This procedure represents both an industrial and scientific method for the

determination of the grinding wheel topography [23–26]. Subsequently, an optical surface measurement is carried out with an InfiniteFocus 3.5 of Alicona Imaging GmbH, Raaba/Graz, Austria. Finally, the roughness values mean arithmetic height Sa, maximum height Sz, reduced peak height Spk and reduced valley depth Svk as well as the grinding specific parameters static number of cutting edges  $N_{stat}$ , cutting edge density  $C_{stat}$  and mean grain protrusion  $k$  are determined using a developed algorithm in Matlab® of The MathWorks, Inc., Natick, Massachusetts, USA. Here,  $N_{stat}$  is the number of cutting edges of the abrasive grains that protrude from the bond per unit area. The grain protrusion  $k$  indicates the height at which the grains protrude from the bond. Furthermore, the cutting edge density  $C_{stat}$  takes this the height into account and thus indicates the number of cutting edges per volume unit [8, 20, 24, 25, 27]. In addition, the accuracy of the imprint method was analysed using a roughness standard prior to the technological tests. Deviations of the roughness values according to ISO 13565 [28] and ISO 4287 [29] were 1% of the stated nominal values of the roughness standard.

## 4 Technological investigations

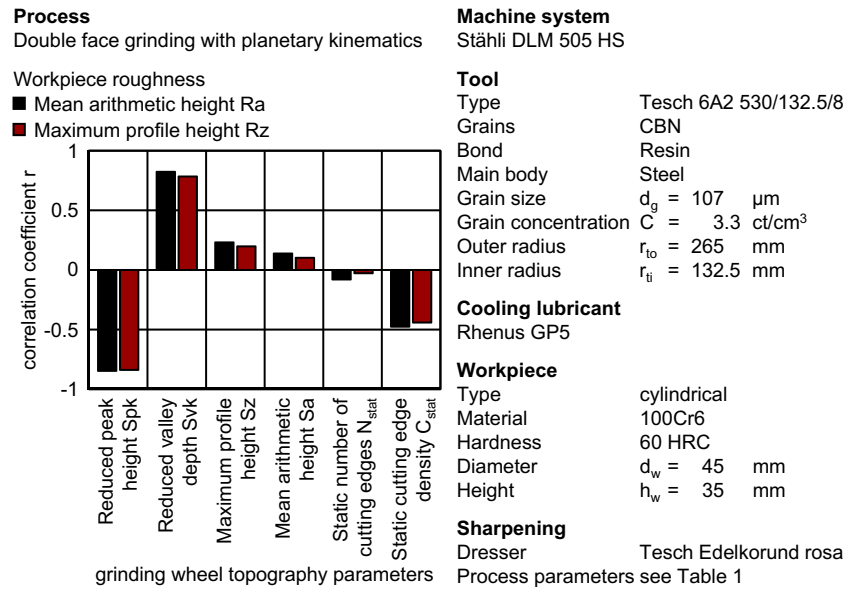
### 4.1 Experimental set-up

Experiments are carried out on a DLM 505 HS machine system from Stähli AG, Pieterlen/Biel, Switzerland. The tools used are resin bonded grinding wheels with specification B107 C75 with twelve radially inserted grooves on a steel

**Table 2** Investigated influencing factors during dressing experiments

| Influencing variable                         | Unit          | Low level | High level |
|--|---------------|-----------|------------|
| Rotational speed of grinding wheels $n_{td}$ | l/min         | 30        | 60         |
| Rotational speed ratio $n_{td}$              | –             | – 0.75    | 0.75       |
| Lubricant flow rate $\dot{V}_{1,d}$          | l/min         | 0         | 45         |
| Dressing process force $F_{pd}$              | daN           | 30        | 90         |
| Machined dresser height $\Delta h_d$         | $\mu\text{m}$ | 500       | 2000       |
| Dresser grain size $d_{gd}$                  | Mesh          | 90        | 180        |

**Fig. 7** Correlation between surface parameters of workpiece and grinding wheel topography



base body from Diamant-Gesellschaft Tesch GmbH, Ludwigsburg, Germany. Grinding tests are performed with cylindrical workpieces made of fully hardened bearing steel 100Cr6 with a hardness of 60 HRC. Both the grinding and the dressing processes are carried out using DP5 grinding oil from Rhenus Lub GmbH & Co KG, Mönchengladbach, Germany. The dressers are made of corundum grain with mesh size 90 and 180 which are held in a porous ceramic bond. In the first step, the grinding wheels are blunted in grinding processes with industrial conventional grinding parameters (Table 1). Here, the blunting criterion is a material removal rate of  $\Delta \dot{h}_w \leq 0.1 \mu\text{m/s}$ .

The grinding wheel topography of this blunted initial state is recorded by imprints and the grinding wheel profiles are determined. A dressing experiment is carried out. After this, imprints and profile measurements are conducted again to determine the grinding wheel topographies and profiles. The differences in profile wear  $h_{tp}$  before and after a dressing test provides information about an improvement or deterioration of the grinding wheel evenness. Additionally, the roughness values mean arithmetic height Ra and maximum profile height Rz of both machined workpieces surfaces before and after dressing are ascertained to draw conclusions about the cutting ability of the grinding wheels. Afterwards, grinding processes are done again until the blunting criterion is reached and a new

dressing process is carried out using the same procedure. Macro- and microscopic wear are recorded using the methods described in Section 3. To determine the significant influencing factors, a mean value comparison of a two-level test is carried out. A two-stage definitive screening design with triple realization and a total number of 96 tests is used here [30, 31]. The influencing factors to be investigated and their values are listed in Table 2. For this purpose, the difference  $\bar{d}$  between the two mean values and the 95%, 99% and 99.9% confidence intervals are determined for each target variable. If the difference  $\bar{d}$  is above the 95 % confidence interval, the effects of an influencing factor are to be evaluated as indifferent. A significant effect can be assumed above the 99% confidence interval. The one-way analysis of variance (ANOVA) is also used. Thereby the  $p$  value indicates the probability with which the null hypothesis ‘factor has no influence’ can be rejected. An effect is considered indifferent if  $p < 0.05$ , significant if  $p < 0.01$  and non-significant if  $p \geq 0.05$  [31, 32].

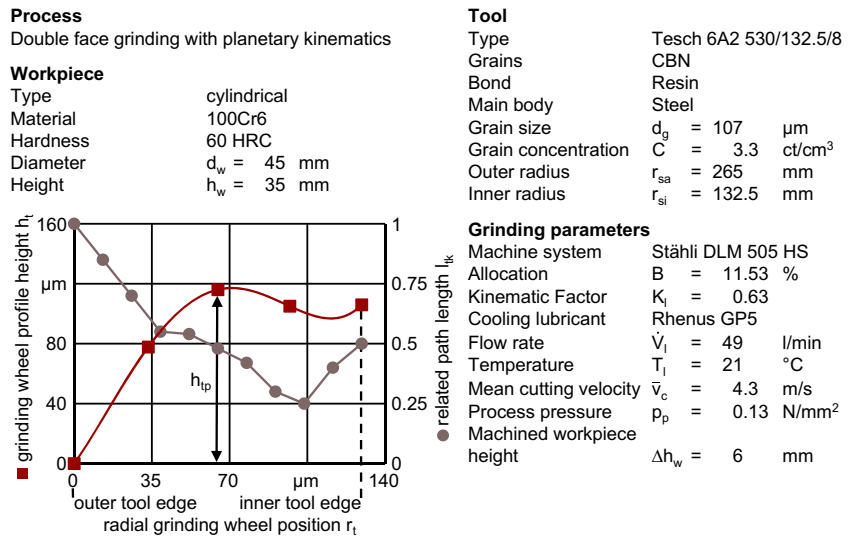
### 4.2 Wear characteristics

The wear condition achieved after blunting is characterized by a 0<sup>th</sup> order profile in negative direction on the lower and upper grinding wheel (Fig. 2). The topography analyses using the imprint method show that a defined initial state was reached before each dressing experiment. Furthermore, the relevant topography parameters of the grinding wheels were determined by a correlation analysis between roughness parameters of the machined workpiece surfaces and the grinding wheel topography parameters. Here, the reduced peak height Spk and the reduced valley depth Svk correlate most strongly with the determined workpiece roughness maximum profile height Rz and mean arithmetic height Ra (Fig. 7). This identification

**Table 3**  $p$  values for the influence of the position on the grinding wheels after grinding and after dressing

|                | Spk   | Svk   | Sa                | Sz                | $N_{stat}$ | $k$   | $C_{stat}$        |
|----------------|-------|-------|-------------------|-------------------|------------|-------|-------------------|
| After grinding | 0.027 | 0.716 | $1 \cdot 10^{-4}$ | $3 \cdot 10^{-4}$ | 0.035      | 0.005 | $6 \cdot 10^{-5}$ |
| After dressing | 0.545 | 0.573 | 0.275             | 0.327             | 0.695      | 0.025 | 0.244             |

**Fig. 8** Wear profile and distribution of the model-based related path length  $l_{ik}$  on the lower grinding tool



of characteristic parameters for describing the influence of the grinding wheel topography on the workpiece surface coincides with previous findings on other grinding processes [24, 26, 27].

The factor ‘position on the grinding wheels’ was tested statistically in a three-stage one-way analysis of variance (Table 3). Here, the determined microscopic wear in the

blunted stage shows a dependence on the ‘inside’, ‘middle’ or ‘outer’ position. The  $p$  values of the effects on grain protrusion  $k$ , roughness  $S_a$  and  $S_z$  are  $p < 0.01$ , thus proving the significance of the position on the grinding wheels. The reduced peak height  $S_{pk}$  and static number of cutting edges  $N_{stat}$  are with a value  $p < 0.05$  in the range of indifference. In contrast, the grinding wheel topographies after the dressing

**Fig. 9** Main effects and double interactions on the profile wear  $h_{tp}$  on the lower grinding wheel

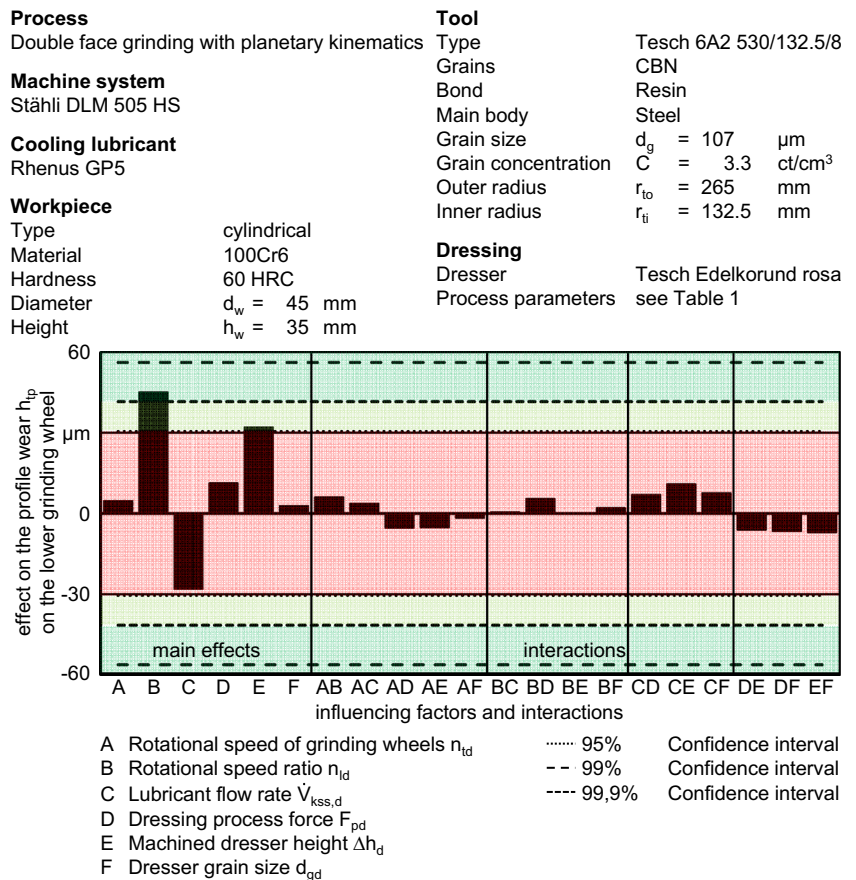
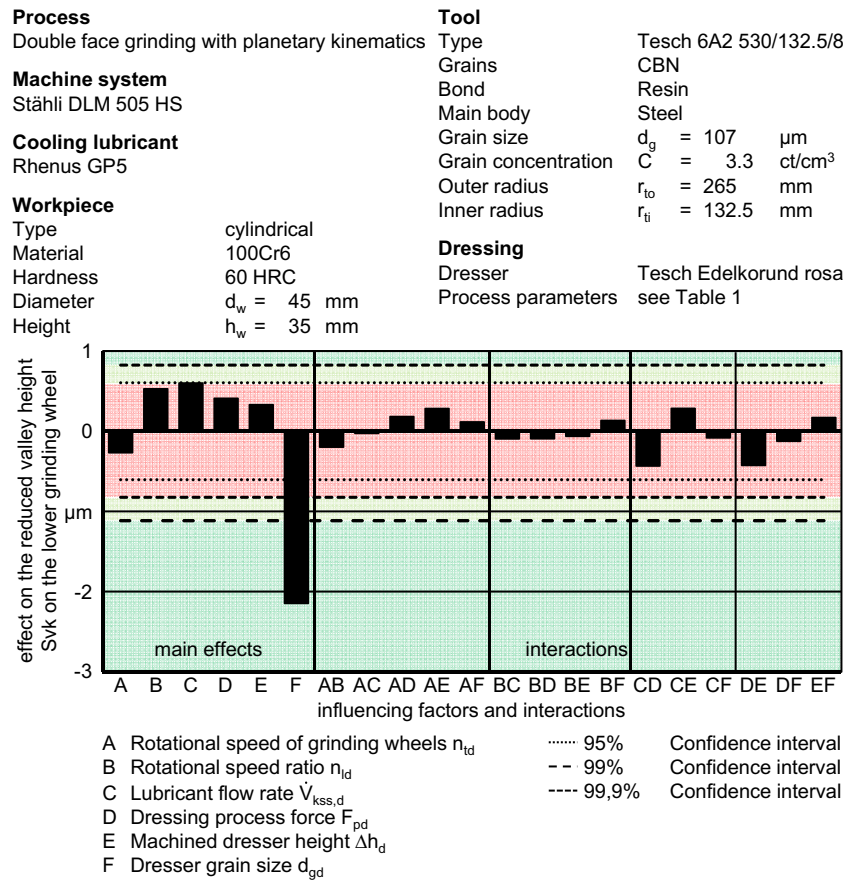


**Fig. 10** Main effects and double interactions on the reduced valley height  $S_{vk}$  on the lower grinding wheel surface



processes show no location dependency. The  $p$  values are all outside the significance level. Only the influence on the grain protrusion  $k$  is indifferent.

The underlying cause is assumed in the process parameters used. Due to the process typical kinematics, the workpieces cover different path lengths in the individual areas of the grinding wheels, and the cutting speed depends on the current workpiece location. Using the kinematic models developed by Simpfendörfer [10], Ardelt [3, 16, 17], Uhlmann et al. [5–7] and List [1], these values can be calculated for the selected process parameters. Here, during grinding the cutting speed difference in the inner and outer area of the grinding wheels is comparatively higher with  $v_{c,diff} = v_{c,max} - v_{c,min} = 1.44 \text{ m/s}$  compared to the difference in the dressing experiments  $v_{cd,diff} = 0.27 \text{ to } 0.70 \text{ m/s}$ . Accordingly, the cutting conditions during dressing are more homogeneous than during grinding and thus, the grinding wheel surfaces generated are also more homogeneous. The inhomogeneous cutting speed  $v_c$  and contact lengths between the workpieces and the different grinding wheel areas during grinding lead to a significant deviation in the investigated topography parameters. On the tool wear model proposed by Uhlmann et al. [6] and List [1], the workpieces cover more than twice as much path length on the outside as on the inside of the grinding wheels in the performed grinding process. The grinding wheel profiles

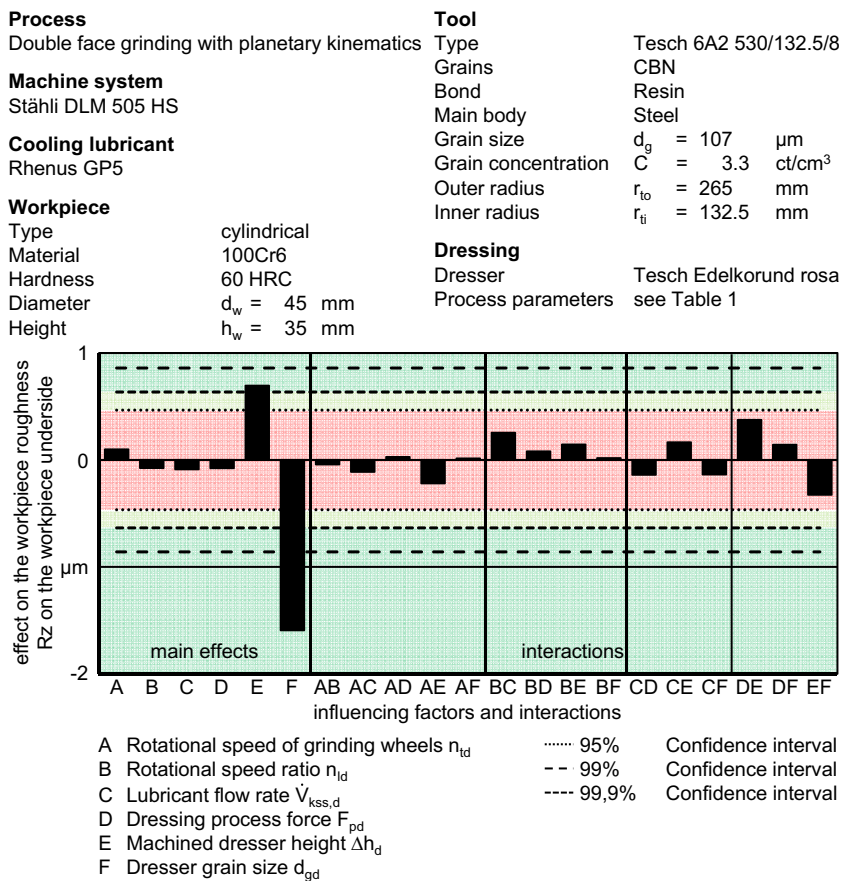
determined after grinding depends on the calculated path length covered by the workpieces in the areas of the grinding wheels (Fig. 8). In the areas with a longer path length, more wear occurs, which results in profile valleys. This leads to the conclusion that the profile wear  $h_{tp}$  is significantly dependent on the frequency of workpiece-to-tool contact in different grinding wheel areas. This finding corresponds to previous observations, according to which the wear profile is influenced by kinematic process parameters [1, 3, 5, 6].

### 4.3 Factors influencing profiling

The effect analysis on the change of profile wear  $\Delta h_{tp}$  at the upper and lower grinding wheel shows that the rotational speed ratio  $n_{id}$  between the inner pin ring and the respective grinding wheel has the largest and significant effect on the profiling process, as exemplarily depicted for the lower grinding wheel in Fig. 9. Here, the rotational speed ratio  $n_{id}$  influences the frequency of the workpieces in each area of a grinding wheel, the cutting speeds  $v_c$  there and thus, the load on the abrasive surface. Its targeted adjustment while profiling can consequently lead to even grinding wheel profiles. The machined dresser height  $\Delta h_d$  shows a smaller and as indifferent classified effect on the profiling result. Considering that at least the profile tips must be cut off to achieve an even



**Fig. 11** Main effects and double interactions on the workpiece roughness R<sub>z</sub> on the lower grinding wheel surface



grinding wheel surfaces, this influencing factor is regarded as relevant. Considering the economic efficiency of profiling, both the machined dresser height  $\Delta h_d$  and the separated volume of the grinding wheels must be minimized. In experiments with a process force of  $F_p = 90 \text{ daN}$ , chattering of the machine was observed, so that an upper limit for the process stability of dressing is assumed here. Dressing processes should therefore be oriented towards the lower tested value of  $F_p = 30 \text{ daN}$ . The variation of the lubricant flow rate  $\dot{V}_{1,d}$  shows no effect on the profile wear on the upper grinding wheel. On the lower one, a higher rate leads to a slight deterioration. It is suspected that the observed increased accumulation of coolant on the lower grinding wheel with a higher lubricant flow rate  $\dot{V}_{1,d}$  leads to an increased outflow of the slurry necessary for the dressing process. As observed, this disturbs the profiling process and the output. A higher grinding wheel speed  $n_s$  has, however, no effect on the lower grinding wheel. On the other hand, it leads to an increment of the profile wear on the upper one. It is assumed that due to the higher rotational speed, the slurry film is interrupted and thus no longer cuts off the grinding layer. In contrast, the greater accumulation of coolant lubricant on the lower grinding wheel ensures that the slurry film does not tear off.

### 4.4 Factors influencing sharpening

The dresser grain size  $d_{gd}$  is identified as a significant influencing factor on the grinding wheel topographies after sharpening. A smaller grain size of  $d_{gd} = 69 \mu\text{m}$  results in a smaller reduced valley depth  $S_{vk}$  (Fig. 10). Contrary to this, the reduced peak height  $Sp_k$  increases. The grinding wheel topographies are thus characterized by more protruding grains with the bond set back. No significant effects on the abrasive layer topographies were found for the other process parameters investigated. Nevertheless, the lubricant flow rate  $\dot{V}_{1,d}$  and the machined dresser height  $\Delta h_d$  are within the range of the indifference of the target value  $C_{stat}$ . Here, a higher lubricant flow rate  $\dot{V}_{1,d}$  has a positive effect on the static cutting edge density  $C_{stat}$ . A possible cause is the lower viscosity and thus the likely better ability of the slurry to reset the bond and remove particles from the grinding wheel surfaces. The effect occurs more strongly on the lower grinding wheel than on the upper one. Due to the horizontal alignment of the grinding wheels, a larger lubricant flow rate  $\dot{V}_{1,d}$  possibly only leads to a change in the slurry behaviour on the lower grinding wheel. On the upper grinding wheel, however, the cooling lubricant drops down continuously, unaffected of the volume supplied.

In relation to the workpiece roughness, the dresser grain size  $d_{gd}$  is also identified as a significant influencing factor (Fig. 11). Here, a smaller grain size leads to smaller roughness values Rz. Furthermore, the machined dresser height  $\Delta h_d$  can be classified as indifferent.

## 5 Conclusion and outlook

The wear condition of the grinding wheels during double face grinding with planetary kinematics can be clearly determined by using a profile measuring system and taking imprints of the grinding wheel surface. Significant factors influencing the sharpening result could be determined by screening tests. The dressing process force  $F_{pd}$  and the rotational speeds of the grinding wheels  $n_t$  could be determined as non-significant influencing factors in the examined parameter space, as long as the process stability is maintained. For profiling, the rotational speed ratio  $n_{1d}$  is the decisive parameter for restoring even grinding wheel profiles. Through specific adjustment in the dressing process, the areas to be levelled can be subjected to greater strain through more frequent dresser-to-tool contacts. Thus, profile heights are cut off and even grinding wheels result. The dresser grain size  $d_{gd}$  was identified as the decisive factor influencing the grinding wheel topography and workpiece roughness. A smaller grain size of  $d_{gd} = 69 \mu\text{m}$  leads to a better resetting of the bond. In this context, the influence of the amount of cooling lubricant supplied and thus the viscosity of the slurry was found to be indifferent. An excessive lubricant flow rate  $\dot{V}_{1,d}$  obviously causes the slurry to be flushed away and thus insufficient dressing ability. Furthermore, the machined dresser height  $d_{gd}$  has an effect on workpiece roughness, grinding wheel topographies and profiles. Since the amount of machined dresser material is crucial for slurry characteristics, the machined dresser height  $d_{gd}$  is identified as relevant influencing factor. In addition, it is affecting the dressing process time  $t_{pd}$  and thus the total load to the wear profile to be levelled. In summary, further investigations of the significant and indifferent influencing factors in a larger parameter space are necessary to analyse combined dressing processes more detailed. Furthermore, analysis of the blunting behaviour over the grinding process time  $t_p$  and the interaction between micro- and macroscopic wear are still pending.

**Authors' contributions** Not applicable

**Funding** Open Access funding enabled and organized by Projekt DEAL. This work was supported by Deutsche Forschungsgemeinschaft e. V. (DFG) (grant number: 354023160).

## Compliance with ethical standards

**Conflicts of interest/competing interests** The authors declare that they have no conflict of interest.

**Data Availability** Not applicable

**Code availability** Not applicable

**Open Access** This article is licensed under a Creative Commons Attribution 4.0 International License, which permits use, sharing, adaptation, distribution and reproduction in any medium or format, as long as you give appropriate credit to the original author(s) and the source, provide a link to the Creative Commons licence, and indicate if changes were made. The images or other third party material in this article are included in the article's Creative Commons licence, unless indicated otherwise in a credit line to the material. If material is not included in the article's Creative Commons licence and your intended use is not permitted by statutory regulation or exceeds the permitted use, you will need to obtain permission directly from the copyright holder. To view a copy of this licence, visit <http://creativecommons.org/licenses/by/4.0/>.

## References

- List M (2019) Ortsabhängiges Verschleißmodell für das Doppelseitenplanschleifen mit Planetenkinematik. In: Uhlmann E (ed) Berichte aus dem Produktionstechnischen Zentrum Berlin. Fraunhofer IRB, Stuttgart
- Uhlmann E, List M, Patraschkov M, Trachta G (2018) A new process design for manufacturing sapphire wafers. *Precis Eng* 53: 146–150. <https://doi.org/10.1016/j.precisioneng.2018.03.011>
- Ardelt T (2001) Einfluss der Relativbewegung auf den Prozess und das Arbeitsergebnis beim Planschleifen mit Planetenkinematik. Dissertation, Technische Universität Berlin. In: Uhlmann E (ed) Berichte aus dem Produktionstechnischen Zentrum Berlin. Fraunhofer, Berlin
- Deja M, List M, Lichtschlag L, Uhlmann E (2019) Thermal and technological aspects of double face grinding of Al<sub>2</sub>O<sub>3</sub> ceramic materials. *Ceram Int* 45(15):19489–19495
- Uhlmann E, Hoghé T (2012) Wear reduction at double face grinding with planetary kinematics. *Prod Eng* 6(3):237–242
- Uhlmann E, Hoghé T, Kleinschnitker M (2013) Grinding wheel wear prediction at double face grinding with planetary kinematics using analytic simulation. *Int J Adv Manuf Technol* 69(9–12): 2315–2321
- Uhlmann E, Kleinschnitker M, Hoghé T (2014) Tool wear model for double face grinding with planetary kinematics. In: Proceedings of the ASME 2014 International Manufacturing Science and Engineering Conference, vol 2, pp 237–242
- Marinescu ID, Hitchiner MP, Uhlmann E, Rowe WB, Inasaki I (2016) Handbook of machining with grinding wheels, 2nd edn. CRC Press, Boca Raton
- Rowe WB (2014) Principles of Modern Grinding Technology. Elsevier Science, Burlington
- Simpfendorfer D (1988) Entwicklung und Verifizierung eines Prozessmodells beim Planlappen mit Zwangsführung. Dissertation, Technische Universität Berlin. In: Spur G (ed) Forschungsberichte für die Praxis. München, Carl Hanser
- Sabotka I (1991) Planlappen Technischer Keramiken. Dissertation, Technische Universität Berlin. In: Spur G (ed) Forschungsberichte für die Praxis. Hanser, München

12. Funck A (1995) Planschleifen mit Läppkinematik. Dissertation, Technische Universität Berlin. In: Spur G (ed) Forschungsberichte für die Praxis. München, Carl Hanser
  13. Stähli AW, Stähli B (2005) Flachhonen und Läppen mit Zweischeiben-Maschinen. Corporate publication Stähli AG, Pieterlen/Biel
  14. Stähli AW (2004) Die Läpp-Technik. Corporate publication Stähli AG, Pieterlen/Biel
  15. Uhlmann E, Kleinschnitker M, Hoghé T (2016) Optimierungspotentiale beim Doppelseitenplanschleifen mit Planetenkinematik. In: Hoffmeister H-W, Denkena B (eds) Jahrbuch Schleifen, Honen, Läppen und Polieren: Verfahren und Maschinen. Vulkan, Essen, pp 67–77
  16. Uhlmann E, Ardelt T, Spur G (1999) Influences of kinematics on the face grinding process on lapping machines. *Ann CIRP* 48(1): 281–284
  17. Uhlmann E, Ardelt T, Spur G (1999) On the effect of path curves on process & wheel wear in grinding on lapping machines. In: Proceedings of the “3rd International Machining & Grinding Conference”
  18. Egger R (2001) Planschleifen von Keramik mit zyklodischer Wirkbewegung. Dissertation, Universität Hannover. In: VDI (ed) Fortschritt-Berichte VDI. VDI, Düsseldorf
  19. Rußner C (2006) Präzisionsplanschleifen von Al<sub>2</sub>O<sub>3</sub>-Keramik unter Produktionsbedingungen [Dissertation]. Technische Universität Dresden, Dresden
  20. Lichtschlag L, Uhlmann E (2020) Schärfprozess beim Doppelseitenplanschleifen: Einflussgrößen des Schärfens beim Doppelseitenplanschleifen mit Planetenkinematik. *wt Werkstattstechnik online* 110(6):393–398
  21. DIN (1984) Prüfplatten; Prüfplatten aus Naturhartstein; Anforderungen; Prüfung, 1st edn. Beuth, Berlin, pp 876–871
  22. Lichtschlag L, Uhlmann E (2019) Profilverschleißreduzierung beim Planschleifen. *wt Werkstattstechnik online* 109(11-12):847–851
  23. Diamant-Gesellschaft Tesch GmbH (2015) Making silicone impressions of grinding wheel layers, Ludwigsburg Available from: <http://www.diamanttesch.de/Making-Silicone-Impressions.pdf>. Accessed 3 April 2019
  24. Uhlmann E, Muthulingam A (2019) Analysis of CNC-controlled block sharpening process of hybrid bonded diamond grinding wheels. In: Proceedings of the 22nd International Symposium on Advances in Abrasive Technology
  25. Hübert C, Mauren F, van der Meer M, Rahman D, Rickens K, Mutlugünes Y et al (2009) Charakterisierung von Schleifscheibentopographien aus fertigungstechnischer Sicht. *Diamant-Hochleistungswerkzeuge* 4:40–47
  26. Hübert C (2012) Schleifen von Hartmetall- und Vollkeramik-Schafffräsern. Dissertation, Technische Universität Berlin. In: Uhlmann E (ed) Berichte aus dem Produktionstechnischen Zentrum Berlin. Fraunhofer, Stuttgart
  27. Sroka F (2005) Konditionieren von Diamantschleifscheiben. Dissertation, Technische Universität Berlin. In: Uhlmann E (ed) Berichte aus dem Produktionstechnischen Zentrum Berlin. Fraunhofer IRB, Stuttgart
  28. Deutsches Institut für Normung e.V (1988) Oberflächenbeschaffenheit: Tastschnittverfahren - Oberflächen mit pletauartigen funktionsrelevanten Eigenschaften: Teil 2: Beschreibung der Höhe mittels linearer Darstellung der Materialanteilkurve, 2nd edn. Beuth, Berlin, pp 13565–13562
  29. Deutsches Institut für Normung e.V (2010) Geometrische Produktspezifikation (GPS) –Oberflächenbeschaffenheit: Tastschnittverfahren – Benennungen, Definitionen und Kenngrößen der Oberflächenbeschaffenheit(4287). Beuth, Berlin
  30. Jones B, Nachtsheim C (2017) Definitive screening designs with added two-level categorical factors. *J Qual Technol*:45(2)
  31. Kleppmann W (2013) Taschenbuch Versuchsplanung: Produkte und Prozesse optimieren. Hanser, München
  32. Siebertz K, van Bebbler D, Hochkirchen T (2010) Statistische Versuchsplanung: Design of Experiments (DoE). Springer, Heidelberg, Dordrecht, London, New York
- Publisher's note** Springer Nature remains neutral with regard to jurisdictional claims in published maps and institutional affiliations.